Petroleum Science 21 (2024) 4376–4390

Contents lists available at ScienceDirect

Petroleum Science

journal homepage: www.keaipublishing.com/en/journals/petroleum-science

Original Paper

An automatic workflow for the quantitative evaluation of bit wear based on computer vision

Dong-Han Yang [a], Xian-Zhi Song [a, c, *], Zhao-Peng Zhu [a, c], Tao Pan [a], Long Tian [b], Lin Zhu [a]

[a] College of Petroleum Engineering, China University of Petroleum (Beijing), Beijing, 102249, China
[b] Engineering Technology Research Institute of Petro China Xinjiang Oilfield Company, Karamay, 834000, Xinjiang, China
[c] State Key Laboratory of Petroleum Resources and Prospecting, China University of Petroleum (Beijing), Beijing, 102249, China

ARTICLE INFO

Article history:
Received 26 July 2023
Received in revised form
6 September 2024
Accepted 21 October 2024
Available online 22 October 2024

Edited by Jia-Jia Fei and Min Li

Keywords:
Bit wear evaluation
Computer vision
Drilling bit information database

ABSTRACT

As global oil exploration ventures into deeper and more complex territories, drilling bit wear and damage have emerged as significant constraints on drilling efficiency and safety. Despite the publication of official bit wear evaluation standards by the International Association of Drill Contractors (IADC), the current lack of quantitative and scientific evaluation techniques means that bit wear assessments rely heavily on engineers' experience. Consequently, forming a standardized database of drilling bit information to underpin the mechanisms of bit wear and facilitate optimal design remains challenging. Therefore, an efficient and quantitative evaluation of bit wear is crucial for optimizing bit performance and improving penetration efficiency.

This paper introduces an automatic standard workflow for the quantitative evaluation of bit wear and the design of a comprehensive bit information database. Initially, a method for acquiring images of worn bits at the drilling site was developed. Subsequently, the wear classification and grading models based on computer vision were established to determine bit status. The wear classification model focuses on the positioning and classification of bit cutters, while the wear grading model quantifies the extent of bit wear. After that, the automatic evaluation method of the bit wear is realized. Additionally, bit wear evaluation software was designed, integrating all necessary functions to assess bit wear in accordance with IADC standards. Finally, a drilling bit database was created by integrating bit wear data, logging data, mud-logging data, and basic drilling bit data.

This workflow represents a novel approach to collecting and analyzing drilling bit information at drilling sites. It holds potential to facilitate the creation of a large-scale information database for the entire lifecycle of drilling bits, marking the inception of intelligent analysis, design, and manufacture of drilling bits, thereby enhancing performance in challenging drilling conditions.

1. Introduction

Nowadays, roller cone bits and polycrystalline diamond compact bits (PDC bits) are ubiquitously employed in the domain of oil drilling. With the continuous optimization and improvement of PDC bit structure design and cutter manufacturing technology, PDC bits have been propelled to an increasingly prominent position within the petroleum drilling market. Compared with traditional roller cone bits, PDC bits offer significant advantages such as high rock-breaking efficiency, long service lifetime, excellent impact, and wear resistance, which can significantly increase the rate of penetration (ROP) for drilling deep and high-pressure wells (Capik and Yilmaz, 2021; Xiong et al., 2020). To optimize PDC bits, numerous experiments have been conducted to simulate the force response, rock breaking mechanism and wear condition of PDC bit during the drilling process. These efforts aim to enhance the material and structural design of PDC bits, ultimately improving their impact and wear resistance (Xiong et al., 2020; Dai et al., 2023). Despite the high impact and wear resistance of PDC bits, cutter wear remains inevitable. When the bit wear reaches a certain threshold, or if any damage occurs to the bit, drilling efficiency significantly decreases, affecting both the duration and cost of drilling operations. Therefore, efficient, and quantitative evaluation

* Corresponding author.
E-mail address: songxz@cup.edu.cn (X.-Z. Song).

https://doi.org/10.1016/j.petsci.2024.10.005

of bit wear condition is crucial for understanding the wear mechanisms and optimizing bit design to ensure efficient and safe drilling (Timonin et al., 2017).

According to the wear characteristics of PDC bits, wear can be categorized into two types: normal wear and abnormal wear. Normal wear occurs when the bit cutter and formation produce continuous or intermittent friction to break the rock. This friction results in micro-cutting, scratching, and rubbing, leading to bit wear and dullness. Typical features of normal wear include continuous groove-like marks on the side and tooth column of the PDC layer in contact with the formation, with cracks being extremely rare in these grooves. Moreover, other PDC layers do not exhibit this delamination phenomenon. Abnormal wear, on the other hand, includes broken cutters (BT), chipped cutters (CT), and lost cutters (LT). These anomalies are primarily caused by factors such as the formation conditions during drilling, design and manufacturing flaws in the bit, or operational errors that result in improper bit functioning (Mazen et al., 2021). Images of various types of worn cutters are shown in Fig. 1.

At present, although the International Association of Drill Contractors (IADC) has established official evaluation standards for drilling bit condition, for the pulled-out bit, the abrasion evaluation and damage analyses still rely on manual measurement and personal experience. Due to the lack of quantitative and scientific evaluation techniques, the results of evaluation are often time-consuming, delayed, subjective, and prone to error. There is a clear need for an innovative, efficient, and intelligent method to assist on-site staff in accurately identifying bit conditions.

Computer vision, as a research field, focuses on endowing machines with the ability to interpret images and videos in a manner analogous to human perception. It involves using cameras and computers to perform tasks such as target identification, tracking, and measurement, effectively replacing human eyes for various graphic tasks. As a scientific discipline, computer vision explores theories and techniques for building artificial intelligence systems that can extract information from images or multidimensional data. AI algorithms in computer vision mimic human vision to interpret, read, and understand visual data, offering automation, high precision, strong universality, and cost-effectiveness. Computer vision has emerged as a crucial constituent in the research of intelligent systems and finds extensive application in manufacturing, transportation, medical, and military fields. However, in the petroleum industry, while computer vision is employed for monitoring site staff behavior and safety detection, its application for recognizing the status of drilling tools is not as prevalent. Specifically, for drilling bits, the unique nature of bit wear and the complexity of evaluation criteria have resulted in a lack of mature, intelligent, and automated methods for identifying bit wear conditions.

In the petroleum industry, a number of companies and universities have embarked on the development of computer vision models with the aim of executing tasks that were conventionally accomplished by human labor. These models find extensive utility in diverse applications, including determining the condition of drilling rigs and enhancing the safety of rig sites.

Chatar et al. (2021) developed a computer vision model capable of determining the status of a drilling rig in real time. Due to the susceptibility of rig sensors to failure, in conjunction with the substantial costs entailed in their maintenance and installation, relying solely on sensor data to ascertain rig status becomes problematic. By proposing a machine learning model that utilizes videos collected from the rig floor to infer rig states, Chatar successfully implemented an effective machine learning pipeline for detecting rig states.

Aldossary et al. (2023) proposed the use of computer vision at drilling sites to enhance the safety of field personnel. Their approach employs real-time object detection techniques in computer vision to detect eight classes of objects: person, helmet colors (red, yellow, blue, and white), head, vest, and glasses. This system automates the real-time detection and monitoring of personal protective equipment (PPE) and employee behavior on-site. By reducing the time required for tracking and creating a safer work environment, this automation can increase worker productivity and safety, while also lowering operational costs.

Furthermore, many companies and universities are developing 2D and 3D computer vision models to understand the relationship between drilling bit design and bit wear.

Taurex Company (Devers et al., 2022) has established an Automatic Metering Laboratory (AML) to implement a digital model and corresponding workflow for analyzing PDC bit wear. Located in the company's central repair and maintenance facility, this system utilizes an automated robotic 3D scan program to scan drilling bits. The scan results are then transmitted to a remote server accessible to engineers for quantifying bit wear. Simultaneously, the results are archived in a relational database to correlate bit wear trends with operation, design, event data recorder (EDR) and other relevant datasets. This comprehensive approach permits an exploration of the intricate relationships among bit design angles, axial and tangential forces, and cutter damage. It enables the identification of inefficient drilling practices underground, thereby promoting enhancements in bit performance.

Halliburton's Oculus system (Forrester, 2022) conducts a comprehensive 3D scan of the drilling bit, which is then uploaded to the bit database. Leveraging bit photos, wear data, and downhole performance data, collected through extensive big data analysis, the system provides a thorough evaluation of the bit. This evaluation is further correlated with the design characteristics of the bit to optimize its performance, including the selection of cutter types at specific locations and the adjustment of cutter angles. Additionally, Halliburton's Cerebro sensors embedded within the bit capture critical downhole data such as lateral and axial vibration, torsional resonance, rotation, stick-slip, weight on bit (WOB), torque, and buckling. These data are instrumental in comprehensively understanding the drilling environment and determining the root causes of bit damage.

Fig. 1. Various types of worn cutters.

Trax Electric Company (Alalsayednassir et al., 2022) has developed a digital system called grA + de for the automatic evaluation of drilling bit wear. The core of the system is machine-controlled, AI-enhanced photogrammetry. Users place the bit into a scanner, approximately a 4-foot cube in size, enabling the system to conduct automatic analysis of the bit. The scanner transforms the physical object into a digital 3D point cloud image. Leveraging this 3D image of the bit, the system offers high precision in assessing the wear of individual cutters on the PDC bit.

UT Austin's automated bit damage evaluation process (Chu et al., 2022) utilizes intelligent algorithms to analyze drilling bit photos captured at rig sites, effectively identifying the root cause of bit damage. Initially, the software uploads a series of photos presenting each blade of the bit, allowing it to identify all the cutters. Subsequently, the software leverages a database of surface sensors and downhole vibration data, alongside rock strength information obtained from adjacent wells, to quantify the damage incurred by each cutter. Finally, employing a classification algorithm, the software determines the average damage for each section of the blade, enabling it to infer the root cause of the bit damage.

Furthermore, computer vision technology is emerging as a valuable tool in various aspects of geological analysis, including rock thin-section identification, rock classification, and particle segmentation. Liu et al. (2022) proposed an intelligent clastic rock thin-section identification technology by constructing a multi-objective recognition network based on CNN + RNN. Xu et al. (2020) utilized convolutional neural networks, specifically ResNet-18, to automatically classify images of metamorphic rocks, igneous rocks, and sedimentary rocks, including clastic and carbonate. In particle segmentation, image processing technology or deep-learning algorithm are employed to segment and extract rock particles while identifying their edge contours (Budennyy et al., 2017; Buono et al., 2019; Pattnaik et al., 2020).

While these methods effectively integrate computer vision into petroleum operations, they do come with limitations. Specifically, the necessity for specialized equipment presents a significant obstacle. For instance, laser scanners, despite their effectiveness, suffer from drawbacks such as heavy weight, large size, and high costs. This impedes their universal deployment at every rig site, especially considering that many rig sites may lack sufficient power and suitable environmental conditions to support such smart equipment.

This paper proposes an automatic standard workflow for quantitative evaluation bit wear and designing a comprehensive bit information database. Initially, the paper develops an image acquisition method for worn bits at drilling sites. Subsequently, leveraging computer vision technology and IADC bit standards, the paper establishes the bit wear classification model and bit wear grading model. These models enable the automatic analysis of bit images, swiftly identifying the degree of wear and type of damage, thereby providing standardized bit status results. Furthermore, the paper translates the developed algorithm into automated software, facilitating quick application at rig sites. This software allows anyone with a phone or camera to capture bit images at the rig site and obtain evaluation results.

This paper introduces a novel approach to collecting and analyzing drilling bit information at rig sites. Through this method, this paper opens up technical prospects to establish a large-scale information database encompassing the entire life cycle of the drilling bit. Such a database can provide data support for researching bit wear mechanisms and personalized optimization designs. Furthermore, this methodology marks the inception of intelligent analysis, design, and manufacturing of drilling bits, thereby enhancing the potential for accelerating progress in drilling challenging formations.

2. The establishment of PDC bit wear evaluation

In this paper, the bit wear classification model and bit wear grading model have been set up. The wear types of bit wear are classified according to IADC standards, defining the criteria for judging the grade of bit wear. For the wear classification model, three types of object detection algorithms are implemented to identify all the cutters on each bit blade, determining their locations and classifying their types. This approach enables the evaluation of the drilling bit condition based on visual cues. The wear classification model can detect various wear characteristics of drilling bits, including no wear feature cutters (NO), wear cutters (WT), broken cutters (BT), chipped cutters (CT), and lost cutters (LT). Regarding the wear grading model, image processing methods are employed to analyze the NO and WT cutters obtained from the preceding algorithms. By analyzing the edge and area of each cutter, the wear grade of the entire drilling bit is identified. The wear grade of each cutter is computed by the cutter's residual diameter according to the IADC standards. In this paper, the cutter wear grading model defines the wear grade by comparing the current area to the original area, with two distinct processing methods outlined.

2.1. The establishment of PDC bit wear classification model

Object detection stands as a fundamental challenge in computer vision, tasked with identifying objects within images and videos, and providing information on their types and positions (Fischler and Rlschlager, 1973). Serving as a cornerstone in computer vision, object detection underpins various other vision tasks, for instance, instance segmentation, image labeling and object tracking. The evolution of object detection algorithms can be delineated into two distinct periods: the period of traditional object detection algorithms (from 1998 to 2014) and the period of deep learning object detection algorithms (from 2014 to present). The progression of object detection algorithms from 2001 to the present is shown in Fig. 2.

Traditional object detection algorithms primarily rely on manual feature extraction, and consist of three main components: region selection, feature extraction and classifier. Initially, candidate regions containing potential objects are selected from the image. Subsequently, object features are extracted from these regions, and the classifier is trained by using these features. However, the region selection strategy based on the sliding window approach requires redundant search, resulting in high computational costs. Moreover, manually designed features limit the model's ability to adapt to complex conditions, leading to suboptimal detection performance and poor model robustness. In recent years, deep learning has revolutionized object detection by automatically extracting data-driven features with robust universality, thus supplanting traditional methods and emerging as the dominant algorithm in the field of object detection.

The object detection algorithms based on deep learning currently include two frameworks: two-stage (Girshick et al., 2014; Girshick, 2015; Ren et al., 2017; He et al., 2017; Cai and Vasconcelos, 2018) and one-stage (Redmon et al., 2016; Redmon and Farhadi, 2018; Bochkovskiy et al., 2020; Solawetz, 2023). In the former framework, candidate boxes of samples are first determined during processing, followed by the utilization of convolutional neural networks (CNNs) for sample classification. The latter framework performs object detection based on specific regression analysis without generating candidate boxes during processing. Comparative analysis shows that the characteristics of these two methods are obviously different. The former is more accurate but exhibits poorer real-time performance, whereas the latter excels in

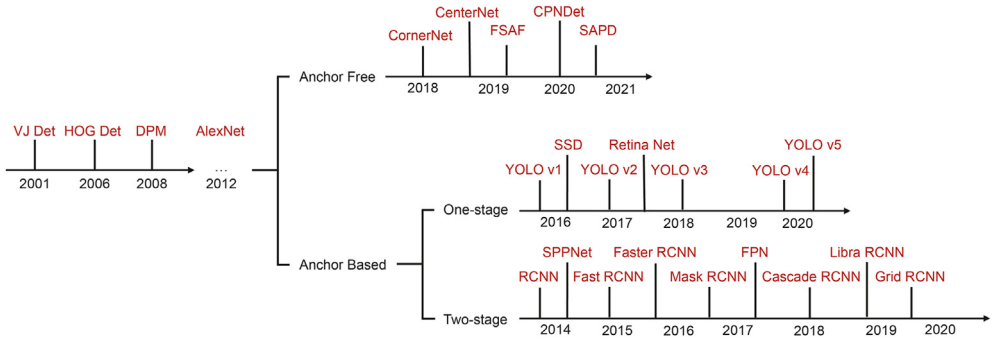

Fig. 2. The progression of object detection algorithms.

detection speed. In recent years, researchers have attempted to migrate Transformer models from nature language process (NLP) into computer vision (CV). Compared with CNNs, Transformer (Dosovitskiy et al., 2020; Liu et al., 2021) can capture internal dependencies within images and leverage contextual information more effectively. Demonstrating versatility across various CV tasks such as image classification, object detection, and image segmentation, Transformer models have showcased significant potential.

For PDC bits, evaluating the type of bit wear involves assessing the condition of each individual bit cutter. Leveraging computer vision, we construct an object detection model to identify and evaluate the condition of each cutter in the bit image. This allows us to determine the wear type of the PDC bit based on the IADC classification standards.

In this experiment, three kinds of PDC bit wear classification models are established based on one-stage, two-stage, and self-attention frameworks. The effectiveness of each model is tested individually. Specifically, these three PDC bit wear classification models respectively refer to the structure of YOLO (Redmon et al., 2016; Redmon and Farhadi, 2018; Bochkovskiy et al., 2020; Solawetz, 2023)-a representative algorithm for the one-stage model, Faster RCNN (Ren et al., 2017)-a representative algorithm for the two-stage model, and Swin transformer (Liu et al., 2021)-a representative algorithm for self-attention models.

The PDC bit wear classification model using the one-stage structure addresses the object detection problem by treating it as a bounding box and classification probability regression task. This model comprises four key components: Input, Backbone, Neck, and Prediction. Input is the module which imports the image and performs initial image processing. Backbone is a convolutional neural network segment that aggregates and synthesizes image features from various fine-grained images. Neck consists of a series of network layers that blend and merge image features before passing them to the prediction layer. Prediction utilizing the image features to predict and generate bounding boxes while classifying categories. The PDC bit wear classification model employing the one-stage structure integrates all modules into a branchless CNN, forming an end-to-end framework. Consequently, the network simplifies due to the absence of branches, leading to significantly faster detection speeds compared to methods relying on candidate regions. The structure of the one-stage PDC bit wear classification model is shown in Fig. 3.

In the one-stage PDC bit wear classification model, the Focus layer and CSP structures are integrated into the Backbone and Neck components. The Focus layer employs a slicing operation to partition a high-definition image (feature map) into multiple low-definition images (feature map). For instance, an original image of $640 \times 640 \times 3$ is input into the Focus structure, which slices it into a $320 \times 320 \times 12$ feature map. Following concatenation, the feature map undergoes another convolution operation, resulting in a $320 \times 320 \times 64$ feature map. The Focus layer converts the w-h plane to the channel dimension and subsequently extracts various features through 3×3 convolution. This approach minimizes the information loss caused by down-sampling. On the other hand, the CSP structure improves the performance of deep neural networks by splitting the input features into two parts and then establishing cross connections between them. This technique effectively improves the feature representation of the model, consequently enhancing its accuracy and generalization ability.

The PDC bit wear classification model using the two-stage structure comprises four key components: Conv layers, Region Proposal Network (RPN), ROI Pooling, Classification and Regression. Conv layers is a feature extraction network that extracts feature maps from images through a sequence of Conv + Relu + Pooling layers, preparing them for subsequent RPN layers and proposals. RPN generates candidate regions, with the aid of bounding box regression, refines these to obtain accurate candidate regions. Then, ROI Pooling gathers the input feature map and candidate regions, synthesizes the information to derive proposal feature maps, and sends them into the subsequent fully connected layer for category determination. Classification and Regression uses the proposal feature maps to classify specific categories and re-applies the bounding box regression to determine the exact final location of the bounding box. The structure of the two-stage PDC bit wear classification model is shown in Fig. 4.

In order to increase the speed of generating proposals in the two-stage model, the RPN is employed to generate proposals directly. The RPN is divided into two parts, one for classifying anchors by softmax to obtain positive and negative classifications, and the other one is used to compute the bounding box regression offsets for anchors to generate accurate proposals. The final proposal layer synthesizes the positive anchors and their corresponding bounding box regression offsets to generate the proposals, Additionally, this layer eliminates proposals that are too small or out of bounds, ensuring that only viable proposals are considered for further processing.

The PDC bit wear classification model using the self-attention with moving windows conspires one patch partition and four stages. Patch partition involves dividing the obtained image into chunks. The four stages are following the patch partition, and each of these stages includes two parts, namely Patch Merging and Swin transformer Block, however, the Patch Merging in the first stage is replaced by a linear layer. Patch Merging is similar to pooling but does not result in information lose that polling does. The Swin transformer Block employs window multi-head self-attention (W-MSA) and shifted-window multi-head self-attention (SW-MSA) to extract information. The structure of the self-attention PDC bit wear classification model is shown in Fig. 5.

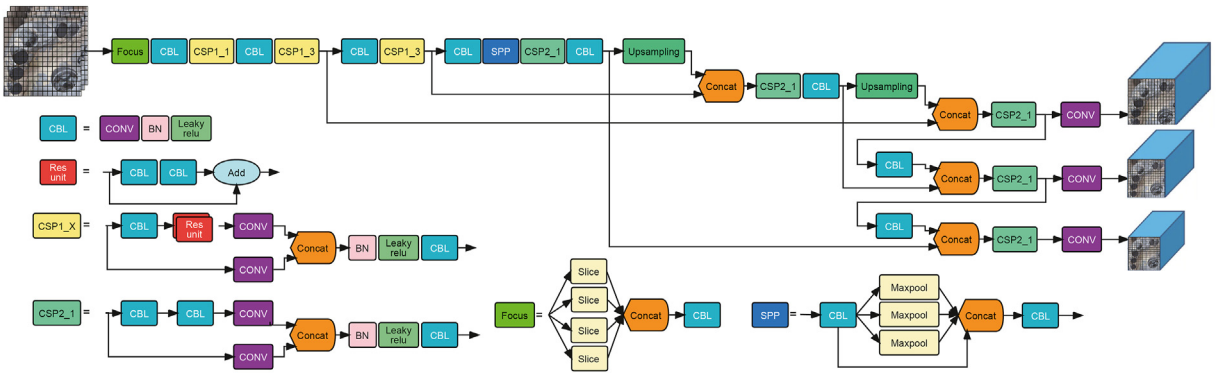

Fig. 3. The structure of the one-stage PDC bit wear classification model.

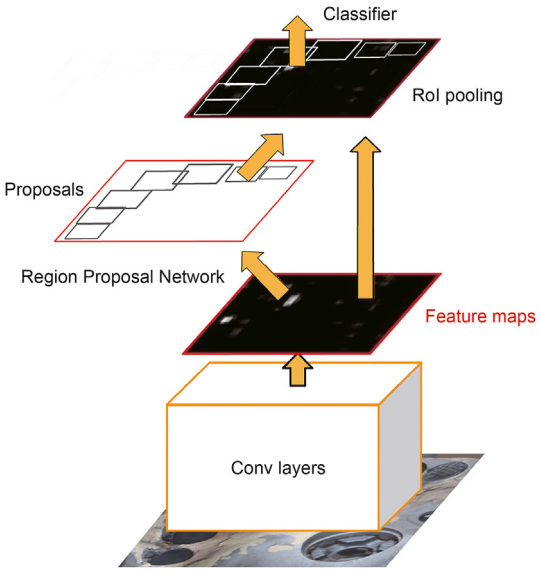

Fig. 4. The structure of the two-stage PDC bit wear classification model.

The method of dividing windows limits the calculation of self-attention (Vaswani et al., 2017) to a local window, and the shifted-window mechanism enhances the relationship between adjacent windows. This approach not only achieves global attention capabilities, but also reduces the computational complexity from a quadratic relationship with image size to a linear relationship. This method significantly reduces the computational load and increases the model speed. In addition, thorough feature fusion, a down-sampling is performed after each feature extraction stage, increasing the receptive field for the subsequent window attention operation on the original image. This allows for multi-scale feature extraction from the input image and hierarchical computation of the feature map, enhancing the model's ability to capture detailed and contextual information.

The commonly used performance evaluation indexes in the field of object detection include accuracy, precision (P), recall (R), confusion matrix, average precision (AP), mean average precision (mAP), precision-recall curve (PR), etc.

P and N indicate that the predicted value is positive sample and negative sample respectively, while T and F indicate that the predicted value is the same or different from the real value. The Confusion Matrix is shown in Table 1.

The precision represents the proportion of positive samples for which the predicted value is correct. Precision is used to measure the accuracy of classifying positive samples by classifier, and the calculation expression is Eq. (1):

$$P = \frac{TP}{TP + FP} \times 100\% \tag{1}$$

To evaluate the performance of a classifier, it's essential to consider not only the precision, but also another evaluation index: recall. Recall measures the proportion of all positive samples correctly predicted by the classifier, reflecting its ability to identify positive samples accurately. The corresponding calculation expression is presented in Eq. (2):

$$R = \frac{TP}{TP + FN} \times 100\% \tag{2}$$

Precision and Recall often exhibit a trade-off relationship, requiring careful consideration to identify the optimal network model during the training process. In general, the precision-recall (PR) curve is used to illustrate the trade-off between precision and recall of the classifier. This curve provides a visual representation of how adjusting the classification threshold affects the precision and recall values, enabling practitioners to select the optimal operating point based on their specific requirements and constraints. By analyzing the PR curve, practitioners can make informed decisions that ultimately optimizing the performance of the classifier for their particular application.

For assessing localization accuracy, this paper uses Intersection over Union (IoU) as an indicator to evaluate the performance of the object detection algorithm. IoU quantifies the degree of overlap between the object prediction frames detected by the algorithm and the real prediction frames labeled within the dataset. It is calculated as the ratio of the area of the overlapping region to the total area encompassed by both frames. The higher the overlap between these two frames, the higher the IoU index. The figure and calculation of IoU is shown in Fig. 6 and Eq. (3).

$$IoU = \frac{A \cap B}{A \cup B} = \frac{TP}{FN + TP + FP} \tag{3}$$

In Eq. (3), A represents the prediction frame, B represents the true frame, the $\cap$ symbol represents the intersection between the two regions of the object prediction frame and the label frame, and the $\cup$ symbol represents the union of the two regions of the prediction frame and the label frame. TP represents the true positive samples, FP represents the false positive samples, TN represents the True Negative samples and FN represents the False Negative samples.

The mAP refers to mean average precision. It is a crucial indicator used to evaluate the performance of object detection

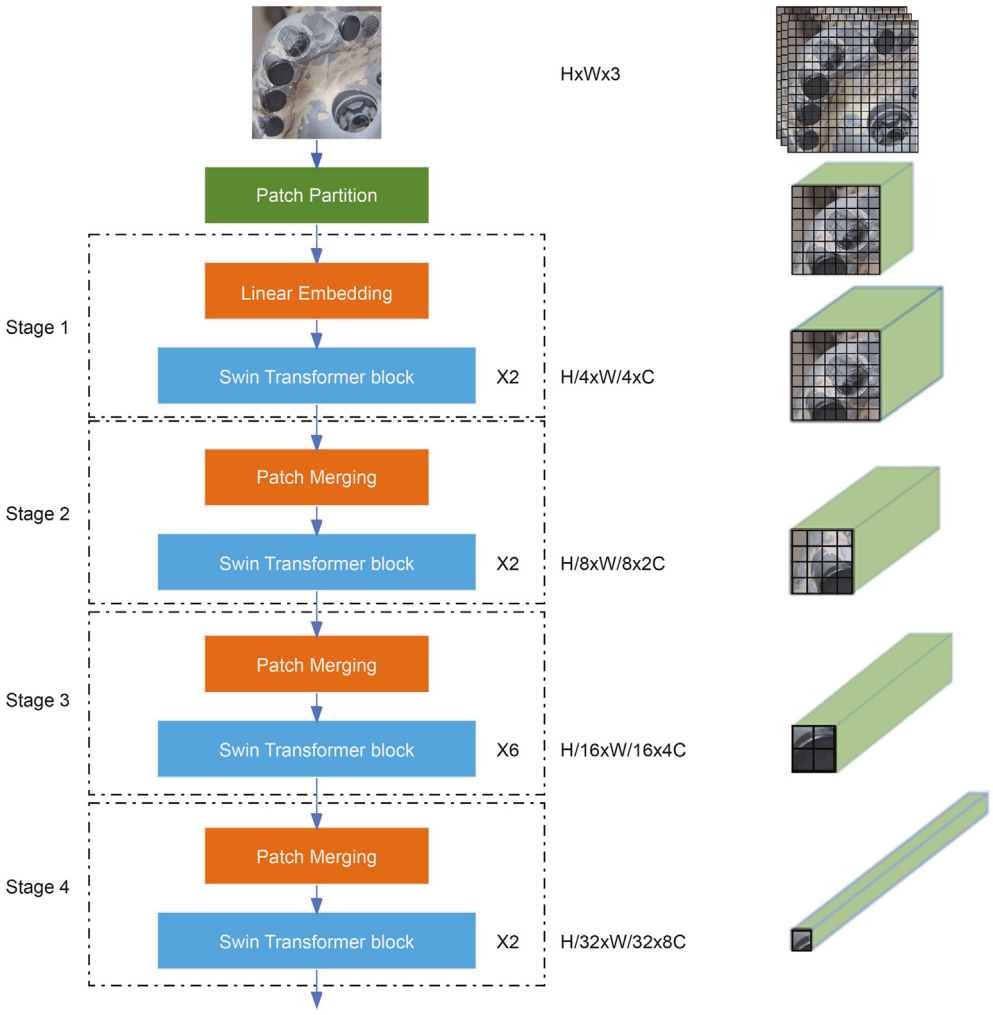

Fig. 5. The structure of the self-attention PDC bit wear classification model.

Table 1
Confusion matrix.

Confusion matrix		Predict	
		P	N
Real	T	True positive, TP	False negative, FN
	F	False positive, FP	True negative, TN

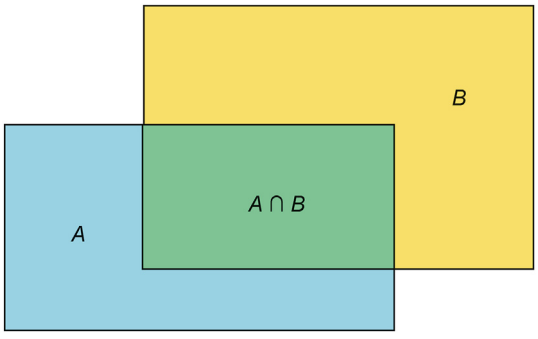

Fig. 6. The figure of Intersection over Union (IoU).

algorithms. In general, mAP represents a comprehensive weighted average of the average accuracy (AP) across all classes of object detection. The corresponding calculation expression for AP is presented in Eq. (4):

$$AP = \int_0^1 P(R)d(R) \times 100\% \tag{4}$$

In Eq. (4), R is the recall, P is the precision.

The corresponding calculation expression for mAP is presented in Eq. (5):

$$mAP = \frac{1}{N}\int_0^1 P(R)dR \times 100\% \tag{5}$$

In Eq. (5), N is the total number of categories, R is the recall, P is the precision.

The mAP@0.5 refers to the mean average precision calculated by all images of all categories when the Intersection over Union (IoU) of the model is set to 0.5. The mAP@0.5:0.95 represents the average value of different IoU threshold ranging from 0.5 to 0.95, with a step size of 0.05. These thresholds include 0.5, 0.55, 0.6, 0.65, 0.7, 0.75, 0.8, 0.85, 0.9 and 0.95, respectively. In this paper, the mAP@0.5 and the mAP@0.5:0.95 will be used as the main indexes to evaluate the performance of the PDC bit wear classification model.

The primary purpose of the object detection model utilized in this paper is to precisely locate and classify the bit cutters by scanning the provided bit images. To enhance the detection accuracy of the models, particularly improving the mean average precision (mAP), the anchor box design has been optimized. This optimization aims to better enable the models to detect the cutters in the images with increased focus and precision.

In the object detection algorithms, anchor box refers to that the algorithm's selection of specific anchor points within an image, using a predetermined step size. Based on these anchor points, reference boxes of varying sizes are generated. Each anchor box encapsulates both the presence possibility and category likelihood of an object. Examples of different anchor box structures are shown in Fig. 7.

Since the size and position of the bit cutters tends to remain relatively consistent within a single drilling bit image, selecting size-matched anchor boxes can enhance both the convergence and accuracy of the model. During the training process, the optimal anchor box size is automatically calculated based on the characteristics of the training set, enabling the model to adaptively determine the length and width of the anchor box.

2.2. The establishment of PDC bit wear grading model

For PDC bit, evaluating the bit wear grade involves measuring the amount of wear on each cutter. At present, the on-site method for determining the grade of wear primarily relies on the height of the worn cutter as the grading basis. According to the IADC standards, the diameter of the cutter is divided into eight segments, using the relative length of the worn diameter to determine the wear grade. Field workers typically use the Vernier caliper to measure the height, which is inefficiency and lacks accuracy. The specific way for PDC bit wear grading based on the diameter is shown in Fig. 8.

In this paper, based on the results from the bit cutter object detection, the precise position of each cutter on the bit blade can be determined. By cropping the image, individual pictures of each cutter can also be obtained. Each individual cutter image is then preprocessed to calculate its current area. Using the wear area, rather than height, to assess the cutter's wear level which allows for more accurate results. Image preprocessing mainly includes image graying, filtering and denoising, threshold segmentation, edge detection, area calculation and so on.

Image graying refers to converting the three-channel color values of each image pixel into a single gray value.

Filtering and denoising refers to the process of removing noise from digital images using filtering algorithm. This reduces the impact of noise and preserves the essential details of the image, resulting in a cleaner and more accurate representation.

Threshold segmentation refers to the division of the image pixel set based on gray levels. Each segmented area corresponds to a region in the actual scene, ensuring that each area has consistent attributes while adjacent areas do not. This process enables the segmentation and classification of image pixels effectively.

Edge detection involves identifying pixels where there is a sudden change in grayscale and then connecting these contiguous edge pixels to form the edges of objects in the image. This process helps in highlighting the boundaries and shapes within the image.

Area calculation refers to the process of determining the size of a closed region in an image by counting the number of pixels within that region. This measurement provides a quantifiable representation of the object's area.

Based on this process, the current area of a single cutter can be obtained. The wear grade of the current cutter can then be calculated by comparing the area with the initial state of the cutter. There are two methods to determine the initial state of the cutter area.

In the first method, during the stage of image acquisition, meticulous control is required to guarantee the acquisition of the original cutter image under the conditions of an identical picture shooting angle and a consistent distance between the camera and the bit. Through the calculation of the digital area of the original cutter and a subsequent comparison with the area of the worn cutter, the current wear grade can be determined. This method emphasizes the significance of standardized imaging conditions for the accurate quantification of cutter wear, as any variation in the

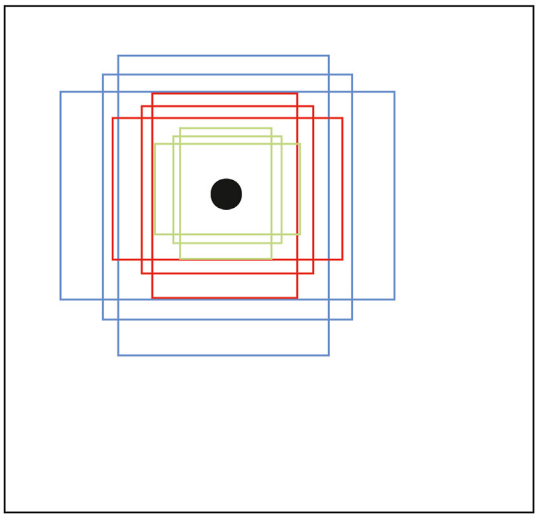

Fig. 7. The different structures of anchor boxes.

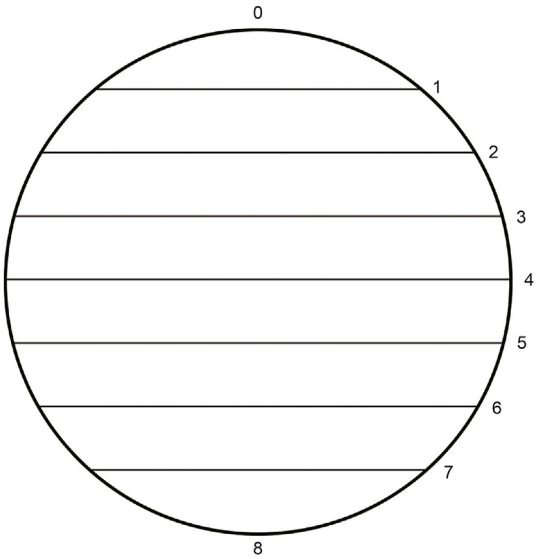

Fig. 8. The diameter wear evaluation criteria according to IADC standards.

shooting angle or camera-bit distance could potentially introduce errors or inaccuracies in the determination of the original cutter area and, consequently, the wear grade.

At the actual rig site, it would be ideal if the original state of the cutter area can be obtained simply and directly by managers. In such instances, the ratio of the initial area to the final area can be calculated by the first method directly. However, there may be cases where the rig site is unable to obtain or overlook obtaining the original state of the cutter. In such scenarios, an alternative method is required to get the original state of the cutter, which is the reason for establishing the second method.

The second method implicates the approximation of an external original ellipse by means of ellipse fitting, which is based on the digital image sample points of the edge of current wear condition. This process aims to deduce the original condition from the current wear state. Through the computation of the area of the fitted ellipse and a subsequent comparison with the area of the calculated worn cutter, the wear grade can be determined. This approach capitalizes on the geometric properties and mathematical relationships inherent in ellipse fitting to reconstruct an approximation of the original cutter, thereby providing an alternative means for assessing cutter wear that is potentially less reliant on direct access to the actual original cutter image.

The area results of the initial cutter and the current cutter obtained by the above two methods are compared to derive the ratio of the current area to the initial area, serving as the residual ratio of the cutter. The residual ratio, in conjunction with the IADC standards, correlates with the eight grades judged by cutter diameter. Consequently, the final wear grade of the current cutter is obtained. By calculating the loss area ratio corresponding to the diameter loss, the wear grade of the specific cutter can be determined by this residual ratio. Thus, the model can provide the results of the bit cutter wear grade evaluation. The wear grades judged by both diameter and area ratio of the cutter are shown in Table 2.

3. Experiment

3.1. Data acquisition and labeling

3.1.1. PDC bit image acquisition process

To ensure the model can be effectively applied, it is crucial to build a dataset that reflects the real conditions of the rig site for training purposes. In this paper, we conducted real-time image acquisition of PDC bits directly at drilling sites. These on-site images were then used to create a comprehensive PDC bit dataset for model training. During the dataset creation process, we aimed to capture a wide variety of bit images, encompassing different types and states, to guarantee the dataset's diversity and robustness.

For PDC bits, determining the wear type and wear degree relies on assessing the state of each bit cutter. From the computer vision perspective, the primary requirement is to capture a clear image of the bit that distinctly shows each blade, enabling the algorithm to accurately identify and analyze all the cutters.

During the image acquisition process, the staff are required to use mobile phones, cameras, or any suitable image acquisition tools to capture images of the PDC bit blade under good lighting conditions and from the proper angle. To ensure high-quality images, it is recommended that the picture be taken perpendicular to each bit blade, which allows for a clear view of the bit profile and the overall cutting shape. Additionally, ensure that the entire blade is fully illuminated by a normal light source to avoid any shadows that could obscure specific details.

The PDC bit pictures of different conditions were obtained from Henan, China. With the right lighting and angles, we photographed approximately 100 drilling bits, resulting in 556 PDC blade images with varying types and states, saved as JPG files. The images were randomly divided into the training set and the test set in an 8:2 ratio, with the training set containing 444 images and the test set containing 112 images. The pictures taken with appropriate lighting and angles at the rig site are shown in Fig. 9.

Table 2
The wear grades judged by cutter diameter and cutter area ratio.

Wear grade	Judged by cutter diameter	Judged by cutter area ratio
0	1 diameter	100%
1	7/8 diameter	92.79%–100%
2	3/4 diameter	80.45%–92.79%
3	5/8 diameter	65.75%–0.45%
4	1/2 diameter	50%–65.75%
5	3/8 diameter	34.25%–50%
6	1/4 diameter	19.55%–34.25%
7	1/8 diameter	7.21%–19.55%
8	0 diameter	0–7.21%

3.1.2. Data annotation

Training object detection algorithms requires manual annotation of the training images. By marking the position and type of the corresponding objects in the images, a set of labeled data can be generated, which is subsequently employed to train the object detection algorithms. This process involves drawing bounding boxes around each object and assigning a label to indicate its class, ensuring that the algorithm learns to recognize and classify objects accurately.

For the obtained bit pictures of different types and states, manual annotation was performed on these pictures using the online tool Make Sense. Each object in the pictures was assigned a bounding box to indicate its location, and corresponding type information was added. Because of the vision sense, for the wear characteristics of drilling bits, our focus in detection was centered around the following cutter conditions: no wear feature cutters (NO), wear cutters (WT), broken cutters (BT), chipped cutters (CT), and lost cutters (LT). The annotations were saved in VOC format, and the storage file format is .xml.

The manual annotation is based on visual eye discrimination and the results of each corresponding drill bit evaluation report provided by the field managers and bit factories, following the IADC standards. However, in combination with the IADC standards, the evaluation of the bit wear characteristics relies on artificial rules, and there is no digital drill bit classification standard. Consequently, it is inevitable that the manual marking dataset of bit wear may contain some flaws. To achieve a more professional labeling of the cutter wear type, the final dataset labels were developed in consultation with experts in the drilling bit field and aligned with the wear regulations in IADC standards. The pictures labeled by Make Sense of cutter positions and wear types are shown in Figs. 10 and 11.

During the data annotation process, an issue known as sample imbalance was identified in the classification of drill wear types, especially for the LT (lost cutters). Sample imbalance refers to the disproportionate quantity of samples across various categories during model training. If this dataset is used to train the model directly without addressing this issue, the model may predominantly focus on classes with more reference labels. Consequently, the network parameters are primarily optimized based on the loss from these abundant classes, leading to low detection accuracy for the underrepresented class with fewer reference labels.

In the current mainstream object detection algorithms, particularly those designed for classification problems, the detection process typically involves generating regions using methods like

Fig. 9. The pictures taken with suitable lighting and angles.

Fig. 10. The pictures after labeled by Make Sense.

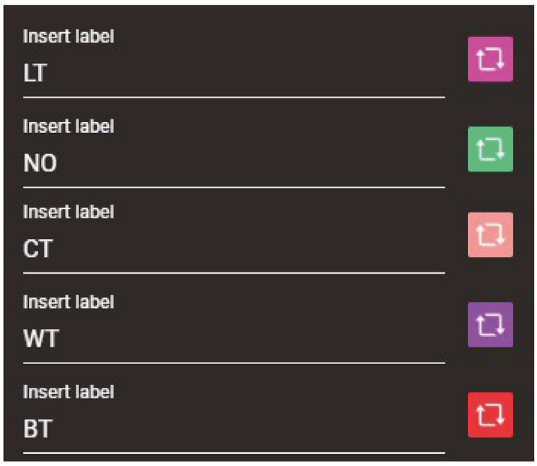

Fig. 11. The colors in the pictures correspond to the wear labels in Make Sense.

RPN (Region Proposal Network), followed by classification and regression for localization within these regions. The presence of sample imbalance issue can significantly diminish the training efficiency and detection accuracy of these models.

To solve this problem, image enhancement methods are introduced to augment the input data, enabling the network model to focus more on learning object features during training process. Common methods include flipping, rotation, and brightness variation, etc., which serve to enrich the dataset and enhance the network's learning capability. Another approach is to overlay information on the image, such as adding noise can enhance the network's ability to detect objects in the presence of interference and poor image quality. These methods effectively mitigate data imbalance problems while simultaneously expanding the dataset and enhancing the model's robustness. The images undergoing the image enhancement methods are shown in Fig. 12.

3.2. The experiment of object detection model

In this paper, all PDC bit images used for model training are sourced from the dataset built previously. In order to facilitate object detection of bit cutters, the dataset comprising 556 images is randomly subjected to the image enhancement methods mentioned above and utilized to train three algorithms established by one-stage, two-stage, and self-attention structures. Throughout the training process, all algorithms undergo 200 epochs with learning rate of 0.005 and batch size of 8, while optimization is performed using the Stochastic Gradient Descent (SGD) method.

In this paper, GPU acceleration is utilized for training. The configurations of both hardware and software resources are shown in Table 3 and Table 4.

All models were implemented using the Pytorch framework, with GPU acceleration facilitating swift training. Here, the mAP@0.5 and mAP@0.5:0.95 values of these three models are shown in Table 5, and the mAP@0.5 curves of these three models with 200 epochs are shown in Fig. 13.

From the mAP@0.5 and mAP@0.5:0.95 of 200 epochs above, it is observed that the one-stage model achieves the highest mAP@0.5, whereas the self-attention model achieves the highest mAP@0.95. Moreover, through the analysis of the mAP@0.5 curves corresponding to each model, it has been determined that the one-stage model manifests a consistently and progressively ascending

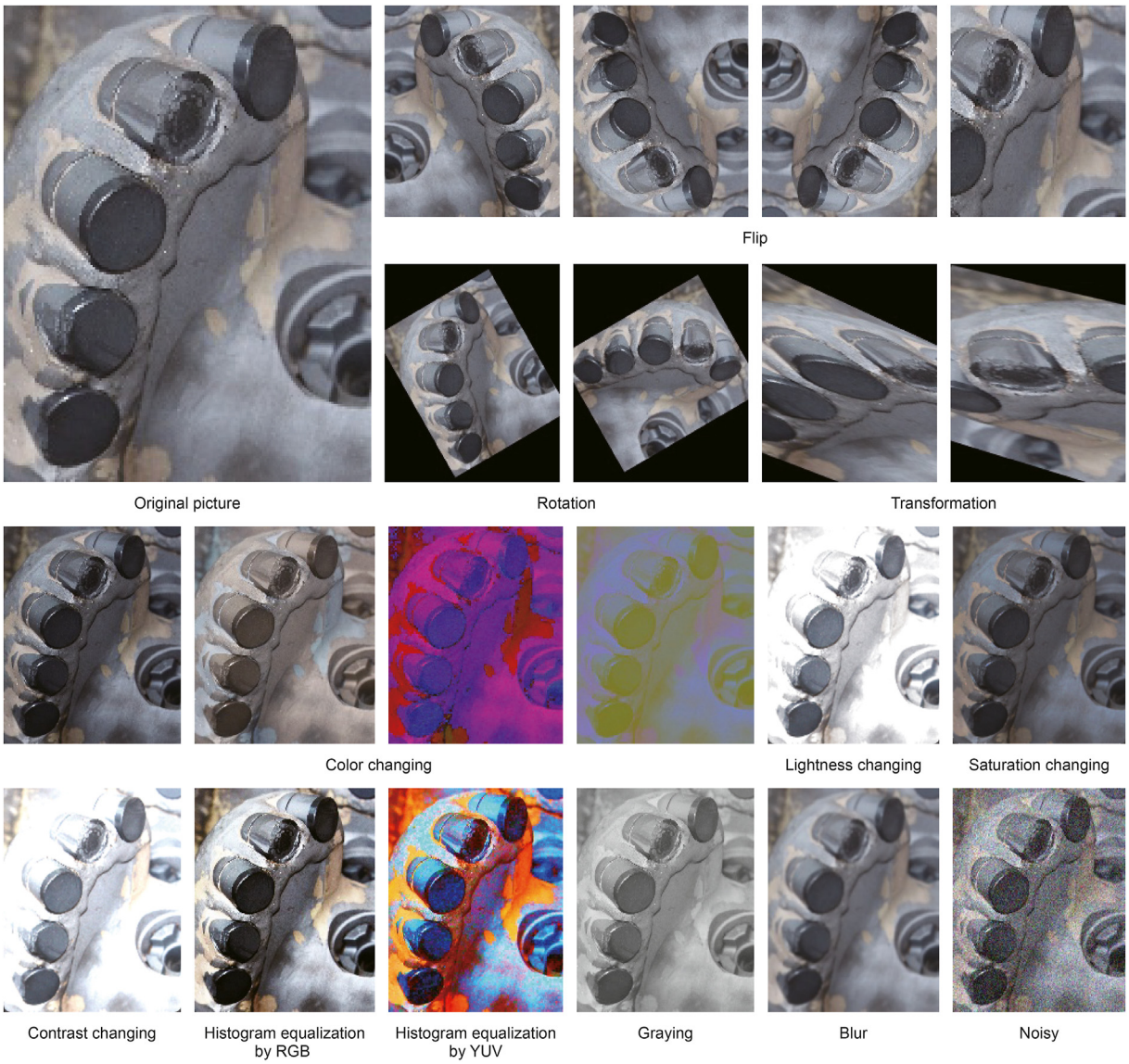

Fig. 12. The images undergoing image enhancement methods.

Table 3
Hardware resource configuration.

Name	Version
CPU	Inter i7 7700K
GPU	GTX1080
RAM	32 GB

Table 4
Software resource configuration.

Name	Version
OS	Window 10
CUDA	10.2
Mmdet	2.11.0
Numpy	1.24.3
OpenCV	4.5.4.58
Pillow	9.0.1
Pycharm	2021.2.2
Python	3.8
Pytorch	1.10.2 + cu102
Torchvision	0.11.3 + cu102
Wheel	0.36.2

trajectory over the 200 epochs and ultimately emerges as the top-performing model with mAP@0.5 value of 70.9. In contrast, when considering the mAP@0.5 results of the two-stage and self-transformer models, which are documented as 64.0 and 67.7 respectively upon the completion of 200 epochs, it can be discerned from the corresponding curves that the principal growth phase predominantly occurs during the incipient stage of training, with the results of 63.78 and 68.952 in merely 25 epochs, implies that the two-stage and self-transformer models might experience a paucity of new information acquisition during the subsequent stage of training.

Therefore, we additionally trained these three models for only 50 epochs. The mAP@0.5 and mAP@0.5:0.95 values of these three models are shown in Table 6, and the mAP@0.5 curves of these three models with 50 epochs are also enlarged in Fig. 14.

From the mAP@0.5 and mAP@0.5:0.95 of 50 epochs above, it's evident that the self-attention model outperforms the others.

Table 5
The mAP@0.5 and mAP@0.5:0.95 values of three PDC bit wear classification models trained by 200 epochs.

Model	mAP@0.5	mAP@0.5:0.95
One-stage model	70.9	55.4
Two-stage model	64.0	52.9
Self-attention model	67.7	56.5

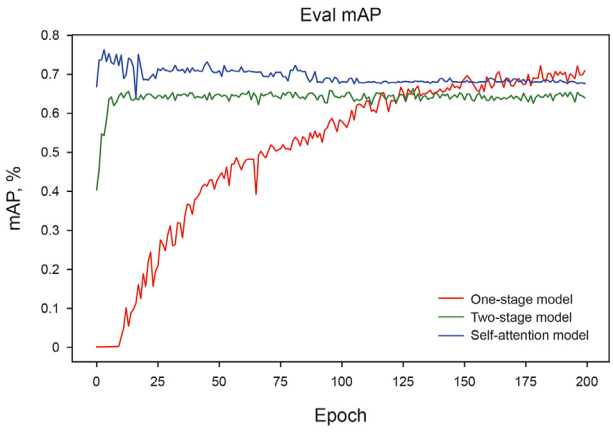

Fig. 13. The curves of mAP@0.5 with epoch change for three models trained by 200 epochs.

Additionally, when observing the mAP@0.5 curves for each model, it's noticeable that while the mAP@0.5 scores of the two-stage and self-attention models stabilize, the one-stage model's mAP@0.5 continues to rise, indicating ongoing learning at this moment.

Simultaneously, data pertaining to the temporal requirements for training the three models over 50 and 200 epochs, along with the time expended for object detection within 100 pictures, were collected. The training and detection time of three models are shown in Table 7 and Table 8.

From the above graphs, it's evident that the one-stage model exhibits the fastest performance in both training and detecting across both 50 and 200 epochs.

Overall, the one-stage model has the highest accuracy and exhibits the fastest training and detecting speeds, especially at high levels of epochs. While the self-attention and two-stage models can attain high mAP in a relatively small number of epochs, and the self-attention model exhibits superior detection results compared to the two-stage model.

After completing the training of these three models, we need to assess the generalization of our model using the test set. We utilize the parameter obtained from the last epoch training on the training set to evaluate its detection capabilities on the test set. Several images were selected and the model was applied to identify the positions and types of bit cutters. The test results are shown in Fig. 15.

Through the test, it is determined that these models can accurately detect the positions of the cutters. While there are slight

Table 6
The mAP@0.5 and mAP@0.5:0.95 values of three PDC bit wear classification models trained by 50 epochs.

Model	mAP@0.5	mAP@0.5:0.95
One-stage model	39.3	26.2
Two-stage model	53.8	39.1
Self-attention model	70.4	43.1

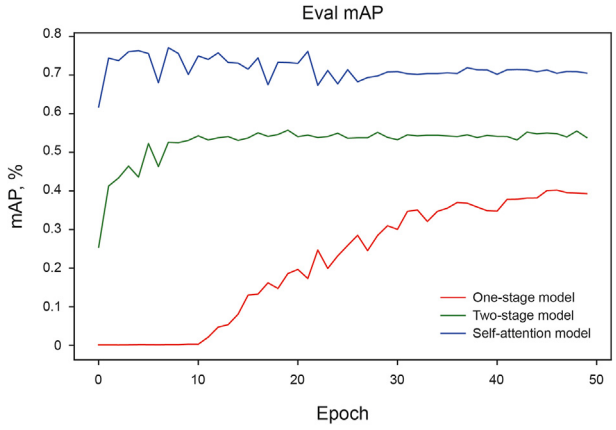

Fig. 14. The curves of mAP@0.5 with epoch change for three models trained by 50 epochs.

variations in the predicted cutter types among the three models, the main results are generally correct. In addition, these models demonstrate the ability to accurately detect cutters across various types, angles, and colors of PDC bits, indicating their robust universality.

In conclusion, the one-stage model demonstrates superior accuracy in both position and type detection, especially under high-epoch training, while also exhibiting the fastest training and detection times. Although the two-stage model exhibits slower training, it still produces good detection results. Moreover, the self-attention model, while the slowest in detecting, achieves commendable detection results. Therefore, each model has its own strengths, but considering practical application in the rig site, prioritizing algorithm efficiency is advisable. Based on this criterion, the one-stage model emerges as the preferred algorithm for bit wear evaluation. However, all three algorithms remain viable options and yield accurate results in real applications.

3.3. The experiment of wear grading model

Firstly, we crop the bit cutter images obtained from the above object detection models according to the detect positions relative to their pictures, resulting in individual cutter images. Then, the PDC bit wear grading model pipeline is utilized to determine the wear grade of each cutter. In this part, the calculation of the cutter area is only performed for two types: no wear feature cutters (NO) and wear cutters (WT), excluding other types such as CT, BT, and LT because they represent abnormal wear. Furthermore, the NO cutters indicate that the cutter remained unworn during this drilling trip. So all NO cutters are assigned to grade 0. Through the image of a single cutter, an image preprocessing pipeline is applied: image graying, filtering and denoising, threshold segmentation and edge detection. This process gives rise to a binary image that distinctly presents the single cutter and its boundary. Through the calculation of the boundary of the single cutter within this binary image, the cutter edge is precisely identified and is then utilized to calculate the current area of the cutter. The cutter images produced by the image preprocessing pipeline are shown in Fig. 16.

After obtaining the current state of the single cutter, we need to estimate its initial state of this cutter using external ellipse fitting. By calculating the wear area of the initial state and comparing it with the current state, we determine the wear proportion. Corresponding to the predefined area grades setting, we can smoothly determine the wear grade of the bit cutter. For example, in Fig. 17, we obtained the current area and the initial area through the

Table 7
The training time of three PDC bit wear classification models.

Model	Training time of 50 epochs, h	Training time of 200 epochs, h
One-stage model	0.5	2
Two-stage model	2.8	11
Self-attention model	1.3	5

Table 8
The detecting time of three PDC bit wear classification models.

Model	Detecting time of 100 pictures, s
One-stage model	4.91
Two-stage model	40.65
Self-attention model	62.85

external ellipse fitting, allowing us to determine the wear proportion and the wear grade of this cutter through the ratio of the two areas.

Alternatively, during the image acquisition process, we can obtain pictures of the original and current cutter by ensuring consistent picture shooting angles and camera distances from the same bit. By calculating the digital picture area of the original and worn cutters, the current wear grade can be determined through comparison. For instance, in Fig. 18, we captured the initial and current pictures of the bit using the same shooting angle and lighting conditions to capture each cutter's change. From these pictures, we can calculate the ratio of the two areas to obtain the wear proportion and determine the wear grade of each cutter.

Through the procedures of image processing and area computation, the area of the current cutter is measured to be 40645.5. When the ellipse fitting method is applied, the fitting area of the original cutter is 49875.92. When the direct comparison method is applied, the actual area of the original cutter is 49163.5. By conducting a comparison of the area of the current cutter with the two aforementioned areas of the original cutter, it is found that the wear grade derived from both methods is uniformly 2.

(a) The one-stage model **(b)** The two-stage model **(c)** The self-attention model

Fig. 15. Test results of three models.

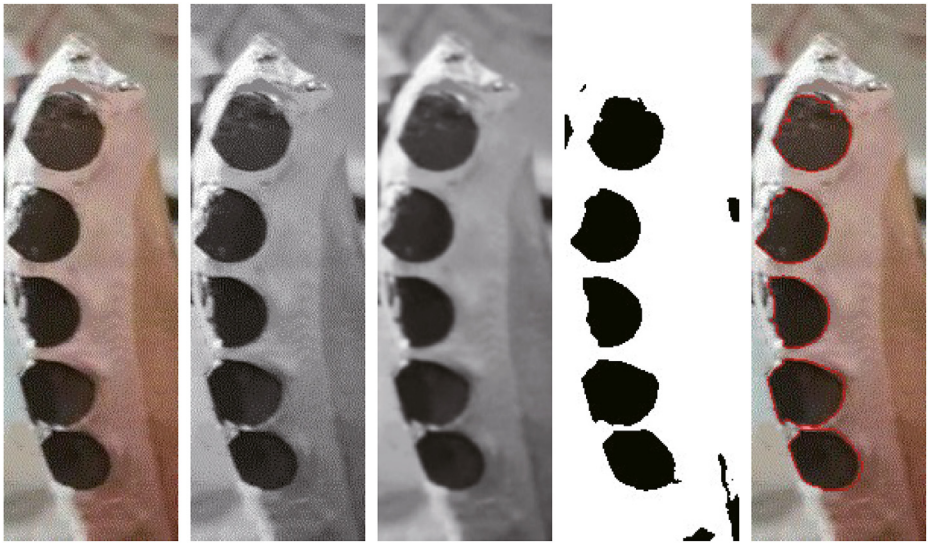

Fig. 16. The cutter pictures through the image preprocessing pipeline.

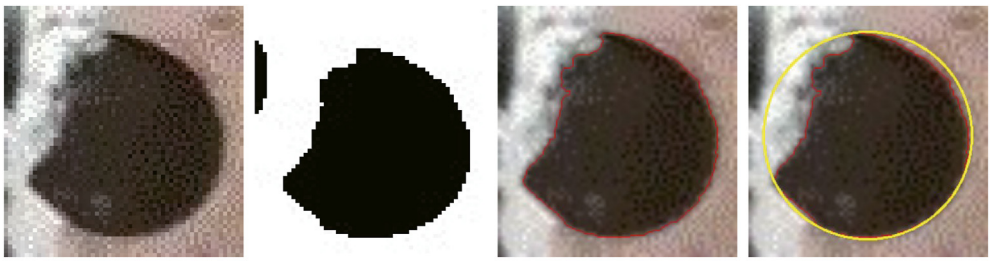

Fig. 17. The results of the ellipse fitting method pipeline.

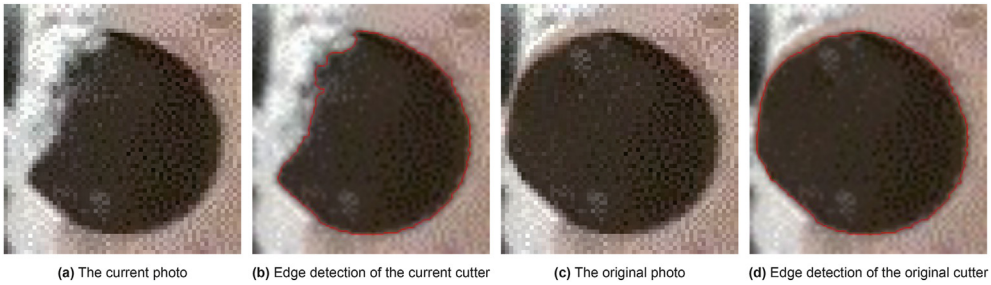

Fig. 18. The results of the direct comparison method pipeline.

3.4. Software implementation

When evaluating the wear condition of the PDC bit, several operations like model selection, parameter setting, input selection, and result display are often necessary. However, object detection algorithms typically consist of code and lack a visual operation interface, making it challenging to perform these operations simply and efficiently. Hence, it is necessary to design a system software that integrates multiple functions. Such software would facilitate automatic and intelligent evaluation of the PDC bit's wear condition, thereby enhancing user operational efficiency.

Based on the analysis of PDC bit wear status process, the system is divided into the following modules.

1 Model selection module: Based on various scenarios and requirements, users may need to choose different algorithm with different accuracy and speed. To accommodate diverse user needs, the model selection module is incorporated, enabling users to select different models according to different requirements and enhancing the universality of the system.
2 Parameter setting module: To accommodate different usage scenarios, the parameters of the network model need to be adjusted accordingly. However, object detection algorithms typically require modification of code files and do not allow for quick parameter adjustment. Therefore, a parameter setting module is designed to enable users to set the model parameters according to different requirements. This simplifies user operations and enhances overall efficiency.
3 Input selection module: To facilitate real-time model calculation based on acquired data, the input selection module allows users to easily and quickly import pictures for model calculation.
4 Result display module: To provide users with a clear view of the model detection and evaluation results, various result display components are integrated. Results are presented using pie charts and other visualizations to facilitate user interpretation.

The PDC bit wear status software interface design and software workflow are shown in Fig. 19 and Fig. 20.

With this software, managers only need to capture pictures of each blade of the drilling bit and import them into the software. The software will then automatically evaluate the wear condition and wear grade of the drilling bit. Through this software and the automatic workflow, wear status results can be obtained at any time using the acquired pictures from the field. This software was tested in Xinjiang, China, and it was found to provide accurate bit wear evaluation results.

4. The design of the drilling bit information database

In this paper, following the acquisition of bit wear evaluation results, a PDC bit lifecycle usage database is designed by integrating bit wear data, logging data, mud-logging data, and drilling bit basic data.

The bit wear data obtained through the above automatic workflow, which corresponds to the IADC standards.

The logging data consists of drilling parameter data for the bit from the beginning to the end of the drilling process. Specific parameters included in the database are Depth, ROP, Hookload, WOB, RPM, PCS, Torque, Inflow_density, Outflow_density, Inflow_rate, Outflow_rate, and Total_pool_volume. All logging data parameters are shown in Table 9.

The mud-logging data corresponds to drilling formation, well track and drilling fluid data during the bit drilling process. Specific parameters included in the database are AZIM, DEVI, GR, RT, SP, AC, DEN, Drilling_fluid_density, and Drilling_fluid_viscosity. All mud-logging data parameters are shown in Table 10.

The drilling bit basic data refers to the type and design parameters of the bit itself. Specific parameters included in the database are Bit_type, Bit_diameter, Footage, Nozzle number, Nozzle diameter, Blade number, and Cutter number. All drilling bit basic data parameters are shown in Table 11.

After obtaining the result of the drilling bit condition, the data is integrated with the logging data, mud-logging data, and drilling bit basic data to obtain PDC bit lifecycle usage data, which is then saved

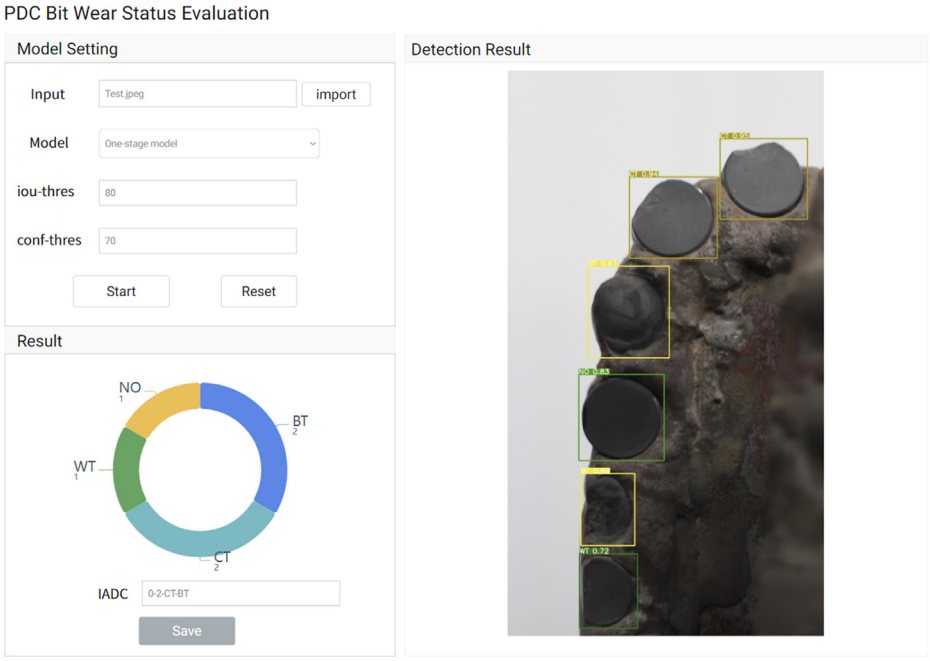

Fig. 19. The software of PDC bit wear status.

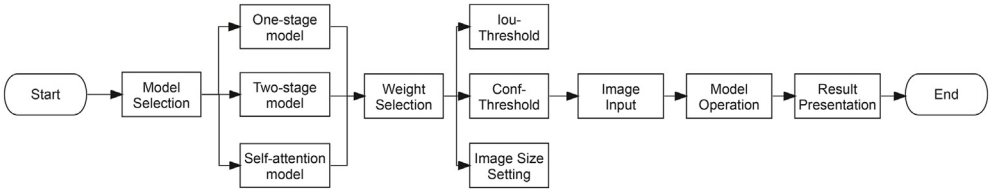

Fig. 20. The software workflow.

Table 9
The parameters in logging data.

Parameter	Type	Unit
Depth	float	m
ROP	float	m/hr
WOB	float	kN
RPM	float	r/min
PCS	float	st/min
Hookload	float	kN
Torque	float	kN·m
Inflow_density	float	g/cm^3
Outflow_density	float	g/cm^3
Inflow_rate	float	L/s
Outflow_rate	float	L/s
Total_pool_volume	float	m^3

Table 10
The parameters in mud-logging data.

Parameter	Type	Unit
AZIM	float	°
DEVI	float	°
GR	float	API
RT	float	Ω·m
SP	float	mv
AC	float	μm/s
DEN	float	g/cm^3
Drilling_fluid_density	float	g/cm^3
Drilling_fluid_viscosity	float	Pa·s

Table 11
The parameters in drilling bit basic data.

Parameter	Type	Unit
Bit_type	string	Null
Bit_diameter	float	mm
Footage	float	m
Nozzle number	int	Null
Nozzle diameter	float	Null
Blade number	int	Null
Cutter number	int	Null

into the database. This database synthesizes the usage records of all drilling bits, providing data support for subsequent intelligent selection, analysis, design, and manufacturing of the drilling bits. This contributes to further unleashing the potential for accelerating progress in drilling challenging formations.

5. Conclusion

PDC bit wear evaluation is an essential method for enhancing drilling site efficiency, improving bit evaluation accuracy, reducing labor costs, and acquiring relevant data.

This paper achieves the entire workflow of the bit wear evaluation, implementing both the PDC bit wear classification model and PDC bit wear grading model. By the structure of one-stage, two-stage, and self-attention, three object detection algorithms are

established to classify bit wear characteristics. Furthermore, two bit wear grading models are devised utilizing the ellipse fitting method and the direct comparison method, leveraging computer vision techniques. With the data acquisition method designed in this paper and the bit image dataset created based on this method, along with the image processing methods, all models demonstrate robust adaptability to various environments and bit types.

In addition, based on the models and algorithms, this paper designs and implements a bit wear status software. This software integrates the above wear classification and wear grading model and has been successfully deployed in Xinjiang, China. It is capable of providing high-quality PDC bit wear evaluation results, thereby fulfilling the requirements of drilling sites. Moreover, based on the obtained PDC bit wear evaluation results, in conjunction with the logging data, mud-logging data, and drilling bit basic data, a PDC bit lifecycle usage database is established. This database will facilitate intelligent selection, analysis, design, and manufacturing of subsequent drilling bits, thereby unleashing the potential for acceleration in drilling challenging formations.

CRediT authorship contribution statement

Dong-Han Yang: Writing – review & editing, Writing – original draft, Visualization, Validation, Software, Methodology, Investigation, Formal analysis, Data curation, Conceptualization. **Xian-Zhi Song:** Writing – review & editing, Writing – original draft, Validation, Supervision, Resources, Project administration, Funding acquisition, Formal analysis, Conceptualization. **Zhao-Peng Zhu:** Writing – review & editing, Writing – original draft, Validation, Supervision, Resources, Project administration, Formal analysis, Conceptualization. **Tao Pan:** Visualization, Validation, Software, Investigation, Data curation. **Long Tian:** Visualization, Validation, Software, Resources. **Lin Zhu:** Visualization, Validation, Software, Data curation.

Declaration of competing interest

The authors declare that they have no known competing financial interests or personal relationships that could have appeared to influence the work reported in this paper.

Acknowledgements

The authors express their appreciation to the National Key Research and Development Project (2019YFA0708300), the Strategic Cooperation Technology Projects of CNPC and CUPB (ZLZX 2020-03), the CNPC Science and Technology Innovation Fund (No. 2022DO02-0308) and the Distinguished Young Foundation of National Natural Science Foundation of China (No. 52125401) for their financial support.

References

Alalsayednassir, A., Berger, P.E., Bergfloedt, C., et al., 2022. AI-Enabled, Automated digital dull bit analysis - field experience. Paper Presented at the International Petroleum Technology Conference, Riyadh, Saudi Arabia. https://doi.org/10.2523/IPTC-22001-EA.

Aldossary, R.S., Almutairi, M.N., Dursun, S., 2023. Personal protective equipment detection using computer vision techniques. Paper Presented at the Gas & Oil Technology Showcase and Conference. UAE, Dubai. https://doi.org/10.2118/214093-MS.

Bochkovskiy, A., Wang, C., Liao, H.M., 2020. YOLOv4: optimal speed and accuracy of object detection. https://doi.org/10.48550/arXiv.2004.10934.

Budennyy, S., Pachezhertsev, A., Bukharev, A., et al., 2017. Image processing and machine learning approaches for petrographic thin section analysis. Paper Presented at the SPE Russian Petroleum Technology Conference, Moscow, Russia. https://doi.org/10.2118/187885-MS.

Buono, A., Fullmer, S., Luck, K., et al., 2019. Quantitative digital petrography: full thin section quantification of pore space and grains. Paper Presented at the SPE Middle East Oil and Gas Show and Conference, Manama, Bahrain. https://doi.org/10.2118/194899-MS.

Cai, Z., Vasconcelos, N., 2018. Cascade R-CNN: delving into high quality object detection. 2018 IEEE/CVF Conference on Computer Vision and Pattern Recognition, Salt Lake City, UT, USA, pp. 6154–6162. https://doi.org/10.1109/CVPR.2018.00644.

Capik, M., Yilmaz, A.O., 2021. Development models for the drill bit lifetime prediction and bit wear types. Int. J. Rock Mech. Min. Sci. 139, 104633. https://doi.org/10.1016/j.ijrmms.2021.104633.

Chatar, C., Suresha, S., Shao, L., et al., 2021. Determining rig state from computer vision analytics. Paper Presented at the SPE/IADC International Drilling Conference and Exhibition. Virtual. https://doi.org/10.2118/204086-MS.

Chu, J., Ashok, P., Witt-Doerring, Y., et al., 2022. Drill bit failure forensics using 2D bit images captured at the rig site. SPE J. 27 (6), 3351–3362. https://doi.org/10.2118/204124-PA.

Dai, X., Huang, Z., Huang, T., et al., 2023. Experimental investigation on the cuttings formation process and its relationship with cutting force in single PDC cutter tests. Petrol. Sci. 20 (3), 1779–1787. https://doi.org/10.1016/j.petsci.2022.10.021.

Dosovitskiy, A., Beyer, L., Kolesnikov, A., et al., 2020. An image is worth 16x16 words: transformers for image recognition at scale. https://doi.org/10.48550/arXiv.2010.11929.

Devers, C., Dyer, W., Lyles, D., 2022. Automated forensic PDC dull analysis enables digital feedback loop. Paper Presented at the SPE Annual Technical Conference and Exhibition, Houston, Texas, USA. https://doi.org/10.2118/210044-MS.

Fischler, M.A., Rlschlager, A.E., 1973. The representation and matching of pictorial structures. IEEE Trans. Comput. C-22 (1), 67–92. https://doi.org/10.1109/T-C.1973.223602.

Forrester, S., 2022. Digital technologies support new workflows in drill bit forensics [EB/OL]. Available: https://drillingcontractor.org/digital-technologies-support-new-workflows-in-drill-bit-forensics-62489.

Girshick, R., Donahue, J., Darrell, T., 2014. Rich feature hierarchies for accurate object detection and semantic segmentation. 2014 IEEE Conference on Computer Vision and Pattern Recognition, Columbus, OH, USA, pp. 580–587. https://doi.org/10.1109/CVPR.2014.81.

Girshick, R., 2015. Fast R-CNN. IEEE International Conference on Computer Vision (ICCV), Santiago, Chile, pp. 1440–1448. https://doi.org/10.1109/ICCV.2015.169.

He, K., Gkioxari, Gollár, D, P., et al., 2017. Mask R-CNN. IEEE International Conference on Computer Vision (ICCV), Venice, Italy., pp. 2980–2988. https://doi.org/10.1109/ICCV.2017.322

Liu, H., Ren, Y., Li, X., et al., 2022. Rock thin-section analysis and identification based on artificial intelligent technique. Petrol. Sci. 19 (4), 1605–1621. https://doi.org/10.1016/j.petsci.2022.03.011.

Liu, Z., Lin, Y., Cao, Y., et al., 2021. Swin transformer: hierarchical vision transformer using shifted windows. 2021 IEEE/CVF International Conference on Computer Vision (ICCV), Montreal, QC, Canada. pp. 9992–10002. doi:10.1109/ICCV48922.2021.00986.

Mazen, A.Z., Rahmanian, N., Mujtaba, I.M., et al., 2021. Effective mechanical specific energy: a new approach for evaluating PDC bit performance and cutters wear. J. Petrol. Sci. Eng. 196, 108030. https://doi.org/10.1016/j.petrol.2020.108030.

Pattnaik, S., Chen, S., Helba, A., et al., 2020. Automatic carbonate rock facies identification with deep learning. Paper Presented at the SPE Annual Technical Conference and Exhibition. Virtual. https://doi.org/10.2118/201673-MS.

Redmon, J., Divvala, S., Girshick, R., et al., 2016. You only look once: unified, real-time object detection. 2016 IEEE Conference on Computer Vision and Pattern Recognition (CVPR), Las Vegas, NV, USA, pp. 779–788. https://doi.org/10.1109/CVPR.2016.91.

Redmon, J., Farhadi, A., 2018. YOLOv3: an incremental improvement. http://arxiv.org/abs/1804.02767.

Ren, S., He, K., Girshick, R., et al., 2017. Faster R-CNN: towards real-time object detection with region proposal networks. IEEE Trans. Pattern Anal. Mach. Intell. 39 (6), 1137–1149. https://doi.org/10.1109/TPAMI.2016.2577031.

Solawetz, J., 2023. What Is Yolov5? A Guide for Beginners. Roboflow Blog [Online]. Available: https://blog.roboflow.com/yolov5-improvements-and-evaluation/.

Timonin, V., Smolentsev, A., Shakhtorin, I.O., et al., 2017. Causes of wear of PDC bits and ways of improving their wear resistance. IOP Conf. Ser. Earth Environ. Sci. https://doi.org/10.1088/1755-1315/53/1/012027.

Vaswani, A., Shazeer, N., Parmar, N., et al., 2017. Attention is all you need. Neural Inf. Process. Syst. https://doi.org/10.48550/arXiv.1706.03762.

Xiong, C., Huang, Z., Yang, R., et al., 2020. Comparative analysis cutting characteristics of stinger PDC cutter and conventional PDC cutter. J. Petrol. Sci. Eng. 189, 106792. https://doi.org/10.1016/j.petrol.2019.106792.

Xu, Y., Dai, Z., Luo, Y., 2020. Research on application of image enhancement technology in automatic recognition of rock thin section. IOP Conf. Ser. Earth Environ. Sci. https://doi.org/10.1088/1755-1315/605/1/012024.